Research Square

Preprints are preliminary reports that have not undergone peer review.
They should not be considered conclusive, used to inform clinical practice,
or referenced by the media as validated information.

Influence of Spreader Dispersion on rumour Propagation in Complex Networks

Madhvi Ramrakhiyani
Dhirubhai Ambani University
Mukesh Tiwari
mukesh_tiwari@dau.ac.in

Dhirubhai Ambani University
Sunitha Vadivel
Dhirubhai Ambani University

Article

Keywords:

Posted Date: September 14th, 2026

DOI: https://doi.org/10.21203/rs.3.rs-10772501/v1

License: This work is licensed under a Creative Commons Attribution 4.0 International License.
Read Full License

Additional Declarations: No competing interests reported.

Influence of Spreader Dispersion on rumour Propagation in Complex Networks

Madhvi Ramrakhiyani[1,+], **Mukesh Tiwari**[1,*,+], **and V Sunitha**[1]

[1]Complex Systems Group, School of Technology, Dhirubhai Ambani University (Formerly DA-IICT), Gandhinagar, Gujarat, 382007, India
[*]mukesh_tiwari@dau.ac.in
[+]these authors contributed equally to this work

ABSTRACT

In social systems, information and misinformation can enter the underlying interaction network through multiple independent sources. Its cumulative reach depends not only on the influence of the sources but also on how they are collectively positioned in the network. Here, we study how the spatial dispersion of multiple initial spreaders influences rumour propagation on complex networks. This setting differs from epidemic spreading because rumour spreaders may become inactive after contacting already informed nodes. Hence, the placement of the initial spreaders affects not only initial coverage but also the timing of deactivation. We consider classical three-state rumour dynamics with interaction-driven stifling and compare dispersion-based initial spreader selection strategies, constructed using farthest-first traversal and a hybrid local-connectivity refinement, with non-dispersion-based strategies. Numerical simulations on Erdös-Rényi, Barabási-Albert and Watts-Strogatz networks, together with six real-world network datasets, show that dispersed initial spreaders generally increase both the final rumour size and the peak fraction of active spreaders. This occurs because dispersion reduces overlap among spreading regions and delays deactivation caused by contacts with already informed nodes. The hybrid strategy, which combines topological separation with local connectivity, typically outperforms degree-based seeding over a broad range of spreading and stifling probabilities. Our results show that in multi-source rumour spreading, a combination of broad separation between the initial spreaders and strong local connectivity is crucial for maximizing rumour reach and intensity.

Introduction

During the past two decades, social media platforms have become one of the primary channels for effectively disseminating information. However, they are also prone to facilitating the rapid spread of misinformation, including misleading and unverified content to large sections of their users. Such content can affect individual decision-making, and in turn, influence collective behavior. The scale and speed of its diffusion have therefore raised concerns about its broader societal consequences, including effects on public trust and collective decision making[1,2].

Empirical studies based on large-scale social media data have revealed distinct structural and temporal patterns in the diffusion of information and misinformation. Early work on online diffusion showed that large cascades are rare, inherently stochastic, and often generated by the cumulative activity of many ordinary users rather than the actions of a small number of highly influential users[3]. In the context of misinformation, false news has been observed to spread faster and more broadly than true news, with the difference particularly pronounced in political news[4]. Misinformation also tends to propagate within polarized and homogeneous user communities, giving rise to echo-chamber-like structures that promote repeated exposure and local reinforcement[5]. During the early stages of diffusion, automated accounts are often disproportionately active in spreading low-credibility content, contributing to its initial amplification and increased visibility before subsequent diffusion is driven mainly by human users[6,7].

Given the collective and stochastic character of information diffusion, a natural question concerns how multiple initial spreaders affect the resulting dynamics, in particular, the extent and intensity of the spread. The problem of identifying a set of initial spreaders that maximizes the overall diffusion size is known as the influence maximization problem[8]. From a theoretical standpoint, the influence maximization problem is NP-hard, and, therefore, approximate approaches are commonly employed. A common strategy is to rank nodes according to a centrality measure and select the top k nodes as initial spreaders. Such measures range from standard structural centralities, such as degree, betweenness, closeness, eigenvector, and coreness, to more involved ranking schemes that incorporate additional structural or dynamical information, such as clustering, voting, gravity, or diffusion-based scores[9–11].

When dynamical processes on networks are initiated from multiple spreaders selected by simple ranking-based schemes, the resulting configurations can suffer from redundancy because nearby spreaders often have strongly overlapping regions of

influence. Consequently, selecting the individually most central nodes does not necessarily yield the most effective multi-source configuration for overall spread. Several studies have shown that introducing dispersion among the initial spreaders, even at the cost of selecting nodes with lower individual centrality, can improve diffusion by increasing the initial coverage of the network and reducing overlap between influence regions of different initial spreaders[11–14]. This limitation of purely ranking-based selection has motivated a variety of decentralized approaches for identifying multiple influential spreaders, including VoteRank, coloring-based methods, percolation-based methods, and community-based strategies designed to reduce overlap among the selected spreaders[15–22].

Studies have also shown that identifying influential spreaders depends not only on network structure but also on the underlying dynamical process[23]. In epidemic spreading, influence is often associated with nodes occupying structurally central or core positions, since such nodes can sustain large-scale transmission when acting as individual sources[12]. In rumour spread, however, highly connected or central nodes do not consistently act as dominant spreaders, since their influence is rapidly diminished by the dynamics itself[24]. Instead, large rumour cascades often emerge from the cumulative activity of nodes that are neither highly central nor readily identifiable by standard centrality measures, highlighting the role of moderate connectivity and hidden spreaders in rumour diffusion[25,26].

In earlier work, we introduced a hybrid refinement of the farthest-first strategy for identifying dispersed influential spreaders[27]. In the present paper, we refer to this refinement as FFiDC. Our motivation for extending this framework to rumour spreading comes from the real-world observation that rumour and misinformation often emerge from multiple independent sources. Although FF and FFiDC were introduced in our earlier work in the context of epidemic spreading, the present study is not a direct repetition of that setting. Rumour spreading dynamics differ in a crucial way, since a spreader stops spreading when it encounters nodes that are already informed. As a result, the spatial arrangement of multiple initial spreaders affects not only the initial coverage of the network but also the rate at which spreaders deactivate through redundant contacts. Closely placed spreaders may quickly create overlapping informed neighbourhoods and thereby accelerate stifling, whereas well-separated spreaders can sustain multiple active fronts for longer. At the same time, excessive separation may place some initial spreaders in poorly connected peripheral regions, limiting their ability to initiate substantial cascades. The central question of this work is therefore whether the dispersion-connectivity tradeoff identified for epidemic spreading continues to hold under rumour-specific interaction-driven stifling. We compare centrality-based, random, and dispersion-based initial-spreader selection strategies in terms of their effect on the final rumour size and the peak fraction of spreaders. Our results show that the advantage of dispersed initial spreaders extends beyond epidemic-type diffusion, but only when dispersion is balanced with sufficient local connectivity. The hybrid FFiDC strategy captures this balance most effectively, improving both the final reach of the rumour and the peak spreading activity across random, scale-free, small-world, and empirical networks, although the strength of the effect depends on the underlying network structure.

Results

We examine the performance of dispersion-based and non-dispersion-based strategies for selecting the initial spreaders by comparing the resulting final rumour size and peak fraction of spreaders. The non-dispersion-based strategies considered here are degree centrality (DC), k-shell centrality (KS), and random selection (Random), whereas the dispersion-based strategies are farthest-first traversal (FF) and its hybrid refinement based on intra-partition degree centrality (FFiDC). Details of the rumour dynamics, selection strategies, and numerical procedure are given in the Methods section.

Network Models

Fig. 1 shows the variation of the effective rumour size $r'(\infty) = r(\infty) - s(0)$, which measures the fraction of nodes in the network that become spreaders during the dynamics beyond the initially selected spreaders, as a function of the initial spreader fraction $s(0)$ on Erdös-Rényi (ER) (Fig. 1(a)), Barabasi-Albert (BA) (Fig. 1(b)) and Watts Strogatz small world networks (WS) (Fig. 1(c)). For consistency, the average degree of the networks is kept the same across all the network models. The spreading probability λ is kept small while the stifling probability δ is kept larger so that spreaders quickly transition to the stifling state rather than continuing to spread for long durations. Across all three network types, the effective average rumour size $\langle r'(\infty)\rangle$ initially increases with the initial spreader fraction $s(0)$, reaches a maximum at an intermediate value, and then decreases for large $s(0)$. For small $s(0)$, only a few spreaders are present initially, and since the value of δ is large, they tend to become stiflers before transmitting the rumour widely. In contrast, when $s(0)$ is large, the pool of ignorants is already substantially reduced, so spreaders are more likely to encounter already informed nodes and become stiflers. Thus, both very small and very large initial spreader fractions are unfavorable for maximizing rumour spread.

The three networks differ structurally, with the ER and BA networks having a relatively smaller average path length, $\langle \ell \rangle = 5.34 \pm 0.012$ and $\langle \ell \rangle = 3.48 \pm 0.01$ respectively. The WS network, in comparison, has an average path length of $\langle \ell \rangle = 11.19 \pm 0.14$. The WS network also has a substantially larger average clustering coefficient $\langle C \rangle = 0.51 \pm 0.003$. Despite these structural differences, FF and FFiDC consistently produce a larger effective rumour size than the other methods over the

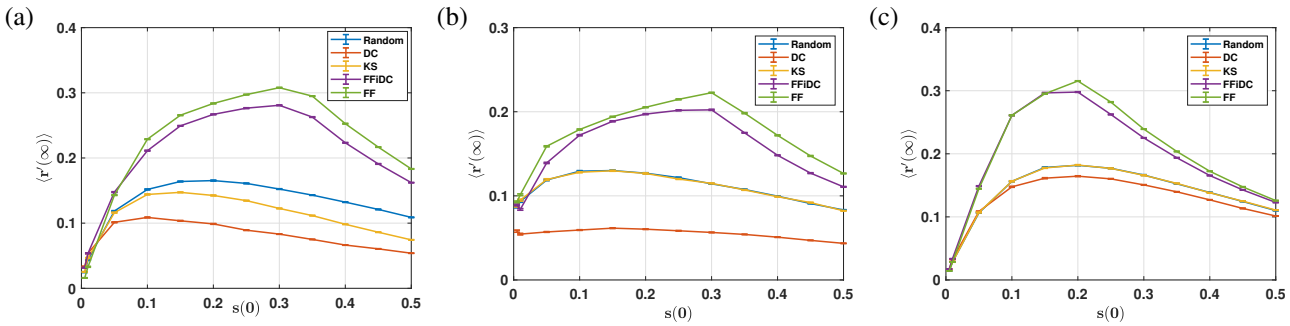


Figure 1. Average final rumour size $\langle r(\infty)\rangle - s(0)$ as a function of the fraction of initial spreaders for (a) Erdös–Rényi random graph, (b) Barabasi-Albert scale free network and (c) Watts Strogatz small world network. The parameter values are $\lambda = 0.1$, and $\delta = 0.5$. The size of the network is 10000 and the average degree is $\langle k\rangle = 6$. For the WS network, the value of rewiring probability $p = 0.05$. Results are averaged over 50 realizations. The error bars show the standard deviation across runs.

intermediate range of $s(0)$. Degree based selection, on the other hand, produces the smallest effective rumour size in all the three cases, with the effect being more pronounced in the BA network. This is consistent with the observation that high-degree nodes in rumour dynamics tend to become stiflers early and act as firewalls to the spreading process[24]. Since these network models do not exhibit a pronounced core-periphery structure, the effective rumour size obtained using KS remains close to the random selection in all three cases.

Figure 2 shows the variation of the effective peak fraction of spreaders $\langle s'_{peak}\rangle = \langle s_{peak}\rangle - s(0)$ as a function of the initial spreader fraction $s(0)$ for the three network models. As in the case of effective rumour size, the effective peak fraction first increases with $s(0)$, reaches a maximum at an intermediate value and then decreases for larger $s(0)$. In all three network models, FF and FFiDC produce larger values of the effective peak fraction over the intermediate range of $s(0)$. In addition, for these two methods, the effective peak fraction remains nonzero over a substantially broader range of $s(0)$, whereas for the other methods it vanishes more rapidly. This can be attributed to the greater spatial separation of the spreaders, which delays overlap between their spreading regions and allows the number of active spreaders to build up more strongly before stifling becomes dominant. By contrast, Random , KS and particularly DC produce much smaller peaks since the selected spreaders are more likely to become deactivated early.

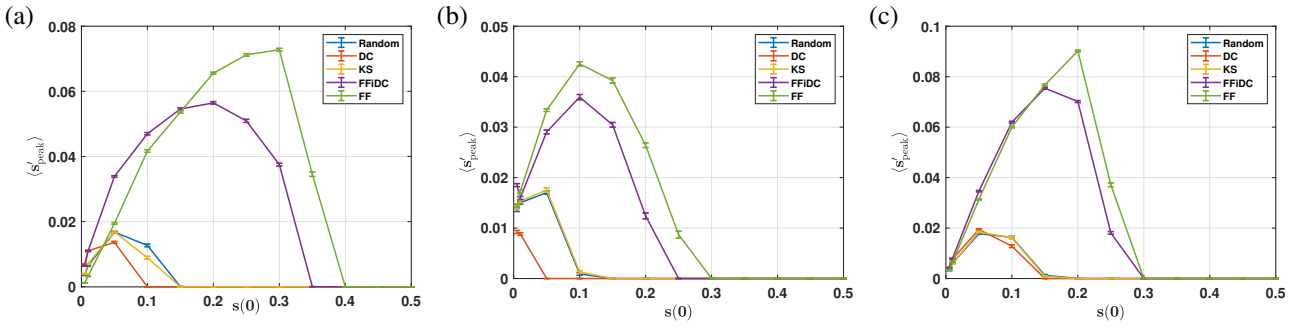


Figure 2. Average value of the peak prevalence $\langle s'_{peak}\rangle = \langle s_{peak}\rangle - s(0)$ as a function of the fraction of initial spreaders for (a) Erdös–Rényi random graph, (b) Barabasi-Albert scale free network and (c) Watts Strogatz small world network. The parameter values are $\lambda = 0.1$, and $\delta = 0.5$). The size of the network is 10000 and the average degree is $\langle k\rangle = 6$. Results are averaged over 50 realizations, and the error bars represent the standard deviation across runs.

Real-world network datasets

The network-model results in the previous section suggest that the role of spreader dispersion is not tied to a particular topology. We further examine the effects of dispersed initial spreaders on six real-world network datasets that differ substantially in size and structural properties. These datasets are Minnesota, Euroroad, US powergrid, E-mail, Political blogs and GRQC, and their key characteristics are summarized in Table 1. Minnesota, Euroroad and US powergrid are spatial networks with large diameter and average path length, whereas E-mail, political blogs, and GRQC have shorter average path length and larger clustering

coefficient. All empirical networks were converted to simple undirected graphs before analysis. Self-loops and multiple edges, if present, were removed. For each dataset, the largest connected component was extracted and used for all simulations. The values of N and E reported in Table 1 correspond to the largest connected component after preprocessing.

Data set	N	E	ρ	C	AC	D	R	$\langle \ell \rangle$
Minnesota	2640	3302	0.00094	0.015	-0.18	99	52	35.34
Euroroad	1039	1305	0.0024	0.0189	0.0900	62	31	18.3
US powergrid	4941	6594	0.0005	0.0801	0.0034	46	23	18.98
E-mail	1133	5451	0.008	0.22	0.07	8	5	3.6
Political blogs	1222	16714	0.022	0.32	-0.22	8	4	2.7
GRQC	4158	13428	0.0015	0.5568	0.63	17	9	6.04

Table 1. Details of the real-world network datasets used in the numerical experiments. Here, N is the number of nodes, E the number of edges, ρ the network density, C the clustering coefficient, AC the assortativity coefficient, D the diameter, R the radius, and $\langle \ell \rangle$ the average path length. The datasets were obtained from the Network Repository (NR)[28]. The size reported here is that of the largest connected component in each dataset.

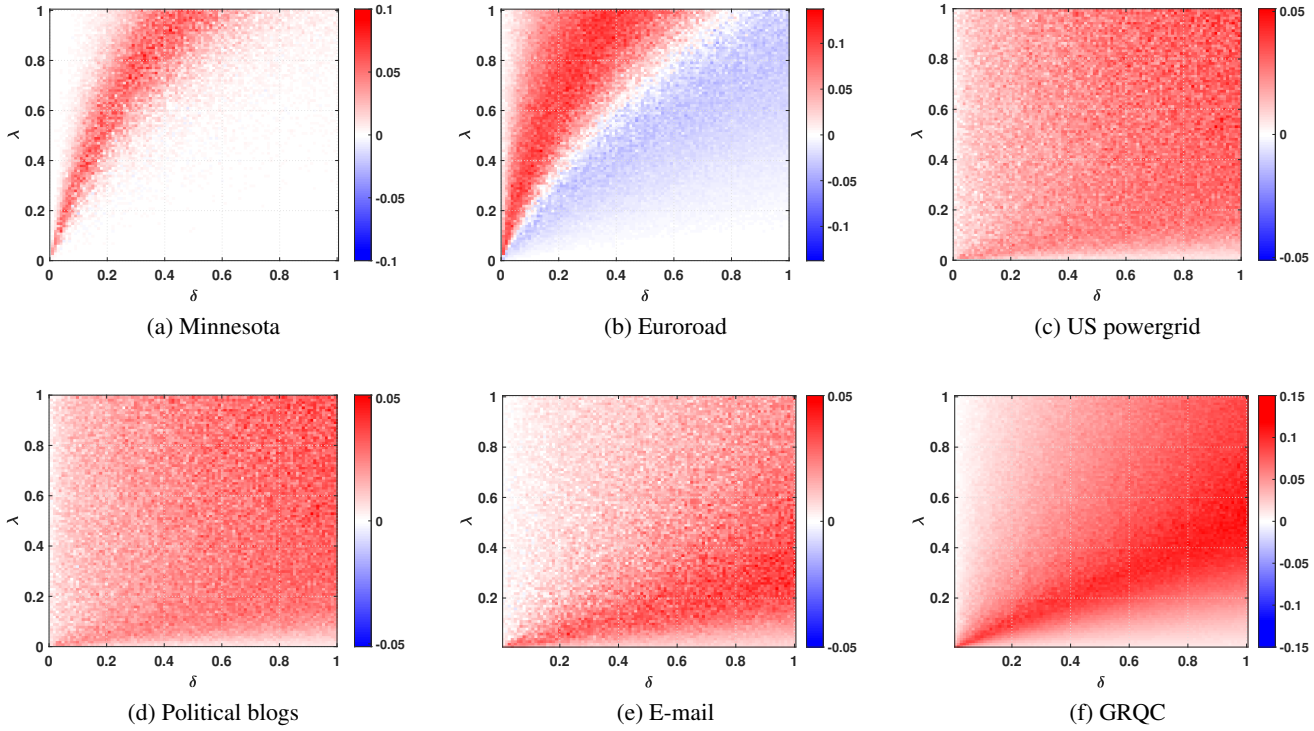
For the real world networks, we focus on FF, DC, and FFiDC since these three methods represent the structural extremes related to our question, namely, maximum dispersion, maximum local centrality, and a hybrid of the two. In addition, we fix the initial fraction of spreaders at 1% ($s(0) = 0.01$). This choice allows us to capture the effects of multiple initial spreaders and at the same time not put DC at an inherent disadvantage. At larger initial fraction, as observed in Figures 1 and 2, FF and FFiDC become increasingly favored in terms of the resulting rumour size and the peak fraction of spreaders. The corresponding values of the average distance between the selected initial spreaders and their average degree are summarized in Table 2.

Table 2. Average pairwise distance between the initial spreaders and average degree of the initial spreaders for different spreader-selection methods across datasets. A visual comparison of the corresponding initial-spreader configurations is provided in Supplementary Fig. S5.

Dataset	Method	Avg. spreader distance	Avg. spreader degree
Minnesota	FF	45 ± 0.75	1.7 ± 0.11
	FFiDC	39 ± 0.90	3.99 ± 0.02
	DC	31.9 ± 2.0	4.04
Euroroad	FF	38.36 ± 1.06	1.17 ± 0.14
	FFiDC	23.02 ± 2.27	5.18 ± 0.46
	DC	6.8 ± 0.11	7.8
US powergrid	FF	26.9 ± 0.30	1.27 ± 0.07
	FFiDC	16.4 ± 0.32	8.74 ± 0.17
	DC	16.08 ± 0.23	11.33
Political blogs	FF	5.1 ± 0.20	2.95 ± 1.88
	FFiDC	2.77 ± 0.24	111.25 ± 28.76
	DC	1.5 ± 0.00	248.42
E-mail	FF	6.1 ± 0.23	1.83 ± 0.72
	FFiDC	2.65 ± 0.15	27.3 ± 2.71
	DC	1.75 ± 0.0	49.54 ± 0.0
GRQC	FF	11.06 ± 0.14	2.02 ± 0.28
	FFiDC	5.69 ± 0.37	18.29 ± 2.40
	DC	1.39 ± 0.04	55.39

As can be seen in Table 2, FF consistently gives the largest average distance between the initial spreaders and the lowest average degree. DC, on the other hand, has the smallest average distance between the initial spreaders and the highest average degree. FFiDC lies between these two extremes, but the extent to which it approaches FF in dispersion or DC in degree varies across datasets. For example, in Minnesota, Euroroad, and US powergrid, the average degree under FFiDC is relatively close to that under DC. The corresponding separation between the initial spreaders, however, differs across these three networks.

In Minnesota and Euroroad, FFiDC retains a much larger average distance than DC, whereas in US powergrid the average distance under FFiDC and DC is nearly the same. In Political blogs, E-mail, and GRQC, the average degree difference between FFiDC and DC is much larger, whereas the difference in the average distance between the initial spreaders is comparatively smaller. This is consistent with the heterogeneous, heavy-tailed degree structure of these networks.



(a) Minnesota (b) Euroroad (c) US powergrid

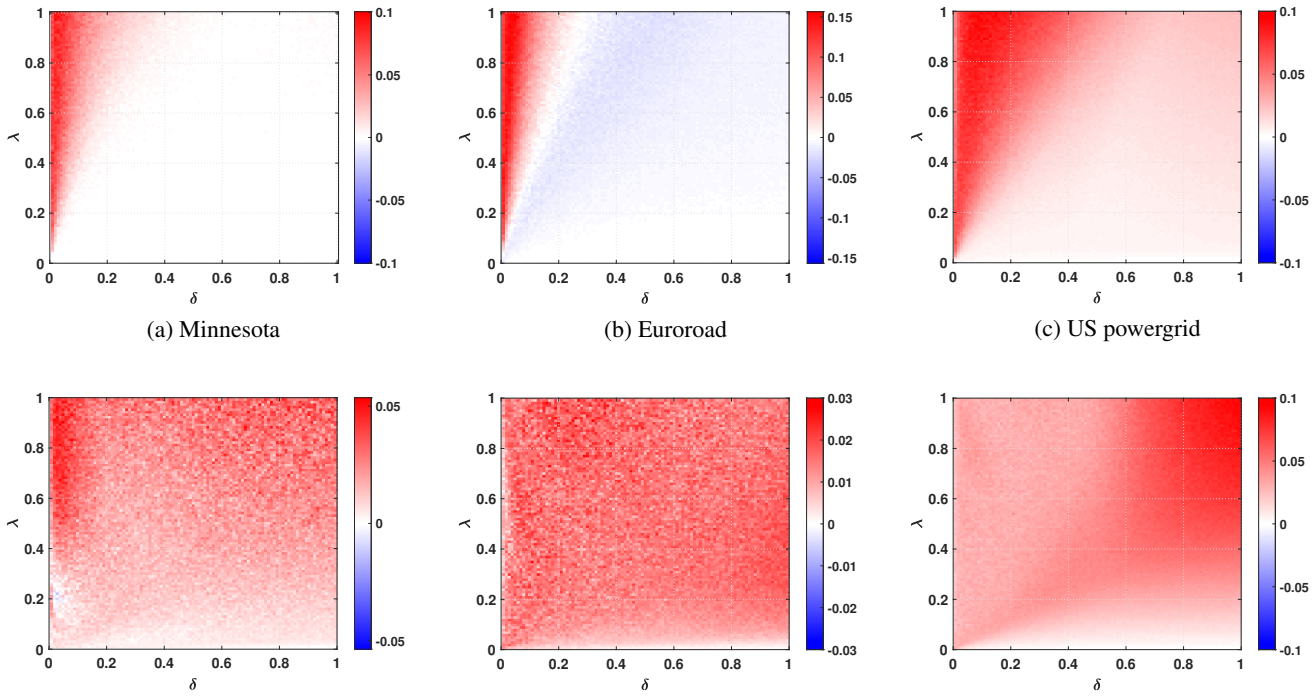
(d) Political blogs (e) E-mail (f) GRQC

Figure 3. Difference in the final rumour size obtained using FFiDC and DC-based initial spreader selection for the different datasets. The fraction of initial spreaders is set to $s(0) = 0.01$. For each combination of spreading and stifling probability values, the final rumour size is computed by averaging over 50 independent realizations. The color bar represents the magnitude of the difference in final rumour size between the two selection strategies.

Figure 3 shows the difference in rumour size between FFiDC and DC $(r_{\mathrm{FFiDC}}(\infty) - r_{\mathrm{DC}}(\infty))$ over the full (λ, δ) parameter plane. The difference in the average rumour size is comparatively smaller in spatial network datasets than in non-spatial datasets. Across all datasets, the difference is low when (λ) and/or (δ) is small. This is expected since in these limiting regimes the outcome depends only weakly on the arrangement of the initial spreaders. When λ is very small, spreaders are unable to transmit widely before turning into stiflers, whereas for very small δ, they remain active long enough so that initial placement matters less. Among all datasets, Euroroad is the only one in which the difference becomes negative, implying that in all other datasets, FFiDC yields a rumour size comparable to or larger than DC across the entire parameter range. The difference between the two is more pronounced in non-spatial datasets, since their heavy-tailed, power-law degree distributions make degree selection more concentrated among hubs, thereby amplifying the firewall effect. The marginally larger rumour size obtained from DC in the Euroroad dataset can be best understood as a small $s(0)$ effect. Because this network is relatively smaller than the other two spatial networks $(N = 1039)$, FFiDC gains part of its initial separation by moving some initial spreaders onto long, sparsely connected peripheral arms. With only 1% of the nodes selected initially, such peripheral placement is not always efficient, since these initial spreaders may fail to trigger substantial cascades before turning into stiflers. By contrast, the DC-selected spreaders, although much less separated, still retain a non-negligible average distance and remain located on better-connected nodes, making them better able to initiate cascades before turning into stiflers. The same tendency is also present in other spatial networks, but because network sizes are larger, the corresponding number of initial spreaders is also larger, and the effect is less visible.

Figure 4 shows the corresponding difference in the peak fraction of spreaders between FFiDC and DC over the full (λ, δ) plane. The overall pattern is similar to that observed for the final rumour size. As in Figure 3, the difference is generally smaller in the spatial networks than in the non-spatial networks. Euroroad is again the only case where a sizeable negative region appears. In the non-spatial dataset the difference is predominantly positive, highlighting the significant effects of dispersed initial spreaders with a high local centrality in small world networks.

The comparison between FF, FFiDC and DC presented in the supplementary material further exemplifies the interplay between initial spreader dispersion, high local centrality and network structure. FFiDC generally gives a larger rumour size than FF in spatial networks, whereas in non-spatial networks, which have smaller average path length and larger degree disparity, the comparison is more mixed. The comparison between FF and DC in the spatial datasets shows behavior similar to that seen for Euroroad in Figure 3(b), with the difference remaining small or changing sign over part of the parameter plane. In the non-spatial datasets, however, FF generally gives a larger average rumour size than DC.



(a) Minnesota (b) Euroroad (c) US powergrid

(d) Political blogs (e) E-mail (f) GRQC

Figure 4. Difference in the average peak fraction of spreaders, $\langle s_{peak} \rangle$, between FFiDC and DC-based initial spreader selection for the different datasets. The initial spreader fraction is $s(0) = 0.01$.For each combination of spreading and stifling probabilities, the peak fraction is averaged over 50 independent realizations. The color bar shows the value of $\langle s_{peak} \rangle$ obtained from the difference between the two selection strategies.

Discussion

In information spreading processes such as rumours, becoming a spreader can happen through exogenous exposure rather than endogenous transmission alone. This makes the multi-source setting especially natural, since a rumour may enter a social network simultaneously at several locations rather than diffuse outward from a single identifiable source. Our study shows that when multiple spreaders are present, the rumour size as well as the peak fraction are not simply determined by how influential these spreaders are individually, but also by how they are arranged collectively. The main picture that emerges is that of a structural tradeoff between initial spreader dispersion and local connectivity. If the initial spreaders are selected solely on the basis of their degree, then they tend to remain concentrated around highly connected parts of the network. This increases overlap among their spreading regions, and in rumour dynamics, can accelerate the transition to the stifler state. At the other extreme, if the initial spreaders are chosen only to maximize separation, some of them may be placed on nodes with weak local connectivity, limiting their ability to trigger substantial cascades. The hybrid refinement, FFiDC, increases rumour size and peak fraction of spreaders because it balances these two effects, preserving the separation achieved by farthest-first selection while avoiding overly peripheral choices. While the effect of the hybrid refinement is visible in both the network models and the real-world datasets, the strength of the effect depends on the underlying network structure. In the non-spatial datasets, the difference between FFiDC and DC is generally more pronounced whereas in the spatial datasets it is weaker, suggesting that locally well-connected initial spreaders are especially effective in networks with short path lengths and strong degree heterogeneity.

Methods

0.1 Rumour Spread Model

In our numerical simulations, we consider the classic rumour spread model implemented on a network of N nodes. At any time t, each node is one of the three states: spreader (S), ignorant I, or stifler R. Spreaders are nodes that are aware of the rumour and actively disseminate it; ignorants are nodes that are unaware of the rumour and stiflers are nodes that are aware of the rumour but have lost interest in propagating it[29,30]. The dynamics evolves through pairwise interactions along network edges. When a spreader contacts an ignorant neighbor, the ignorant becomes a spreader with probability λ, whereas, when a spreader contacts a neighbor that is already informed (spreader or stifler) it becomes a stifler with probability δ. These transitions are represented as:

$$S+I \xrightarrow{\lambda} 2S, \quad S+S \xrightarrow{\delta} S+R, \quad S+R \xrightarrow{\delta} 2R \tag{1}$$

with $S(t)+I(t)+R(t)=N$. The spreader, ignorant and stifler fraction at any time is given as $s(t)=S(t)/N$, $i(t)=I(t)/N$ and $r(t)=R(t)/N$, respectively. Two update schemes are commonly used to simulate rumour dynamics on networks[24]: the contact process (CP) and the truncated process (TP). In the CP, at each time step, every spreader contacts one of its neighbors chosen at random. In the TP, each spreader sequentially contacts all its neighbors in random order unless it becomes a stifler. In our numerical simulations, we have used the TP scheme. However, our key observations are not sensitive to the selected method.

0.2 Farthest First Traversal (FF) and Farthest First traversal with intra-partition Degree Centrality (FFiDC)

The Farthest First Traversal (FF) algorithm, which is the key idea behind identifying initial spreaders here, selects nodes sequentially so as to maximize their topological separation. The first node is chosen arbitrarily, and each subsequent node is selected such that its shortest-path distance to the nearest node in the previously selected set is maximized[31,32]. For instance, in the toy example shown in Fig. 5 (a), starting from the initial spreader, labeled node 11 selected randomly, the algorithm selects nodes 24 and 8 in the two subsequent iterations, respectively. It is noteworthy that this procedure naturally introduces spatial dispersion among the selected spreaders, since each new spreader is chosen to be as far away as possible from the existing spreader set. For example, in networks exhibiting core-periphery structure, such a mechanism often results in early selections occurring in distant peripheral regions, since these are typically far apart in terms of geodesic distance. However, this can also be a limitation for dynamical processes on networks, since peripheral nodes do not necessarily possess strong local connectivity. In Fig. 5(a), nodes 8 and 24 are both located at the periphery and have a degree of 1. In spreading processes, such FF spreaders located at the periphery do not always maximize the reach, especially if the number of initial spreaders is too low or the stifling probability is large.

To include strong local influence in the spreader selection, we proposed a hybrid method that combines FF with locally well-connected nodes, termed FFiDC (Farthest First traversal with intra-partition Degree Centrality). The details of the method can be found in[27], here we briefly outline the main steps. As shown in Fig. 5(b), starting with each FF node as center we first create partitions by assigning every node in the network to the cluster corresponding to its nearest FF node in terms of shortest-path distance. In the case of a tie, the node is assigned randomly to one of the nearest FF-node partition. In Fig. 5 (b), for example, the node labeled 14 is at a distance 2 from both nodes 6 and 21. In this instance, it is randomly assigned to the partition centered at node 6. Within each partition, node with the highest intra-partition degree centrality is assigned to the FFiDC initial spreader set. We also show in Fig. 5 (c), the set of nodes that would be selected if initial spreaders were chosen solely on the basis of degree centrality. In that case, nodes 1, 11, and 21, which are adjacent to each other are selected as initial spreaders. Thus, a purely degree-based strategy tends to concentrate the initial spreaders within the same locally dense region, whereas, FFiDC preserves the spatial dispersion introduced by farthest-first procedure while still selecting locally influential nodes within each partition.

0.3 Performance Metrics

We compare the peak prevalence and the size of the rumour obtained through FF and FFiDC method discussed above with those resulting from standard centrality-based spreader selection strategies. Specifically, we consider degree centrality (DC), in which nodes with the largest degrees are selected as initial spreaders, k-shell centrality (KS), where nodes are ranked according to their coreness in the k-core decomposition and those belonging to the innermost core are chosen as initial spreaders, and random selection in which initial spreaders are selected uniformly at random. We quantify the spreading performance using two standard observables. The first is the final rumour size, $r(\infty)$, defined as the final fraction of nodes that have heard the rumour by the end of the dynamics. The second observable is the peak fraction of spreaders, denoted by s_{peak}, which is the maximum value of the spreader fraction $s(t)$ attained during the evolution. While $r(\infty)$ captures the overall extent of rumour propagation, s_{peak} characterizes the largest instantaneous activity level of the spreading process.

References

1. World Economic Forum. The global risks report 2026 (2026).
2. Lazer, D. M. J. *et al.* The science of fake news. *Science* **359**, 1094–1096, DOI: 10.1126/science.aao2998 (2018).
3. Bakshy, E., Hofman, J. M., Mason, W. A. & Watts, D. J. Everyone's an influencer: Quantifying influence on Twitter. In *Proceedings of the Fourth ACM International Conference on Web Search and Data Mining*, WSDM '11, 65–74, DOI: 10.1145/1935826.1935845 (Association for Computing Machinery, New York, NY, USA, 2011).
4. Vosoughi, S., Roy, D. & Aral, S. The spread of true and false news online. *Science* **359**, 1146–1151, DOI: 10.1126/science.aap9559 (2018).
5. Del Vicario, M. *et al.* The spreading of misinformation online. *Proc. Natl. Acad. Sci. United States Am.* **113**, 554–559, DOI: 10.1073/pnas.1517441113 (2016).
6. Shao, C. *et al.* The spread of low-credibility content by social bots. *Nat. Commun.* **9**, 4787, DOI: 10.1038/s41467-018-06930-7 (2018).
7. Bovet, A. & Makse, H. A. Influence of fake news in Twitter during the 2016 US presidential election. *Nat. Commun.* **10**, 7, DOI: 10.1038/s41467-018-07761-2 (2019).
8. Kempe, D., Kleinberg, J. & Tardos, É. Maximizing the spread of influence through a social network. In *Proceedings of the Ninth ACM SIGKDD International Conference on Knowledge Discovery and Data Mining*, KDD '03, 137–146, DOI: 10.1145/956750.956769 (Association for Computing Machinery, New York, NY, USA, 2003).
9. Pastor-Satorras, R. & Vespignani, A. Immunization of complex networks. *Phys. Rev. E* **65**, 036104, DOI: 10.1103/PhysRevE.65.036104 (2002).
10. Barthélemy, M., Barrat, A., Pastor-Satorras, R. & Vespignani, A. Velocity and hierarchical spread of epidemic outbreaks in scale-free networks. *Phys. Rev. Lett.* **92**, 178701, DOI: 10.1103/PhysRevLett.92.178701 (2004).
11. Zhang, J.-X., Chen, D.-B., Dong, Q. & Zhao, Z.-D. Identifying a set of influential spreaders in complex networks. *Sci. Reports* **6**, 27823, DOI: 10.1038/srep27823 (2016).
12. Kitsak, M. *et al.* Identification of influential spreaders in complex networks. *Nat. Phys.* **6**, 888–893, DOI: 10.1038/nphys1746 (2010).
13. Hu, Z.-L., Liu, J.-G., Yang, G.-Y. & Ren, Z.-M. Effects of the distance among multiple spreaders on the spreading. *Europhys. Lett.* **106**, 18002, DOI: 10.1209/0295-5075/106/18002 (2014).
14. Li, T., Liu, M., Zhang, Z. & Luo, L. Identifying multiple influential spreaders in complex networks by considering the dispersion of nodes. *Front. Phys.* **9**, 766615, DOI: 10.3389/fphy.2021.766615 (2022).
15. Zhao, X.-Y., Huang, B., Tang, M., Zhang, H.-F. & Chen, D.-B. Identifying effective multiple spreaders by coloring complex networks. *Europhys. Lett.* **108**, 68005, DOI: 10.1209/0295-5075/108/68005 (2014).
16. He, J.-L., Fu, Y. & Chen, D.-B. A novel top-k strategy for influence maximization in complex networks with community structure. *PLOS ONE* **10**, e0145283, DOI: 10.1371/journal.pone.0145283 (2015).
17. Ji, S., Lü, L., Yeung, C. H. & Hu, Y. Effective spreading from multiple leaders identified by percolation in the susceptible-infected-recovered (SIR) model. *New J. Phys.* **19**, 073020, DOI: 10.1088/1367-2630/aa76b0 (2017).
18. Liu, D., Jing, Y., Zhao, J., Wang, W. & Song, G. A fast and efficient algorithm for mining top-k nodes in complex networks. *Sci. Reports* **7**, 43330, DOI: 10.1038/srep43330 (2017).
19. Shang, J., Zhou, S., Li, X., Liu, L. & Wu, H. CoFIM: A community-based framework for influence maximization on large-scale networks. *Knowledge-Based Syst.* **117**, 88–100, DOI: 10.1016/j.knosys.2016.09.029 (2017).
20. Ghalmane, Z., Cherifi, C., Cherifi, H. & El Hassouni, M. Centrality in complex networks with overlapping community structure. *Sci. Reports* **9**, 10133, DOI: 10.1038/s41598-019-46507-y (2019).
21. Kazemzadeh, F., Safaei, A. A. & Mirzarezaee, M. Influence maximization in social networks using effective community detection. *Phys. A: Stat. Mech. its Appl.* **598**, 127314, DOI: 10.1016/j.physa.2022.127314 (2022).
22. Rajeh, S. & Cherifi, H. Ranking influential nodes in complex networks with community structure. *PLOS ONE* **17**, e0273610, DOI: 10.1371/journal.pone.0273610 (2022).
23. de Arruda, G. F. *et al.* Role of centrality for the identification of influential spreaders in complex networks. *Phys. Rev. E* **90**, 032812, DOI: 10.1103/PhysRevE.90.032812 (2014).

24. Borge-Holthoefer, J. & Moreno, Y. Absence of influential spreaders in rumor dynamics. *Phys. Rev. E* **85**, 026116, DOI: 10.1103/PhysRevE.85.026116 (2012).

25. Borge-Holthoefer, J., Meloni, S., Gonçalves, B. & Moreno, Y. Emergence of influential spreaders in modified rumor models. *J. Stat. Phys.* **151**, 383–393, DOI: 10.1007/s10955-012-0595-6 (2013).

26. Baños, R. A., Borge-Holthoefer, J. & Moreno, Y. The role of hidden influentials in the diffusion of online information cascades. *EPJ Data Sci.* **2**, 6, DOI: 10.1140/epjds18 (2013).

27. Ramrakhiyani, M., Tiwari, M. & Sunitha, V. Influence of multiple spreaders through farthest first traversal. *Appl. Netw. Sci.* **9**, 70, DOI: 10.1007/s41109-024-00676-6 (2024).

28. Rossi, R. A. & Ahmed, N. K. The network data repository with interactive graph analytics and visualization. In *Proceedings of the AAAI Conference on Artificial Intelligence*, vol. 29, DOI: 10.1609/aaai.v29i1.9277 (2015).

29. Daley, D. J. & Kendall, D. G. Stochastic rumours. *IMA J. Appl. Math.* **1**, 42–55, DOI: 10.1093/imamat/1.1.42 (1965).

30. Maki, D. P. & Thompson, M. *Mathematical Models and Applications: With Emphasis on the Social, Life, and Management Sciences* (Prentice Hall, Englewood Cliffs, NJ, 1973).

31. Rosenkrantz, D. J., Stearns, R. E. & Lewis, P. M. I. An analysis of several heuristics for the traveling salesman problem. *SIAM J. on Comput.* **6**, 563–581, DOI: 10.1137/0206041 (1977).

32. García-Díaz, J., Pérez-Sansalvador, J. C., Rodríguez-Henríquez, L. M. X. & Cornejo-Acosta, J. A. Burning graphs through farthest-first traversal. *IEEE Access* **10**, 30395–30404, DOI: 10.1109/ACCESS.2022.3159695 (2022).

Author contributions statement

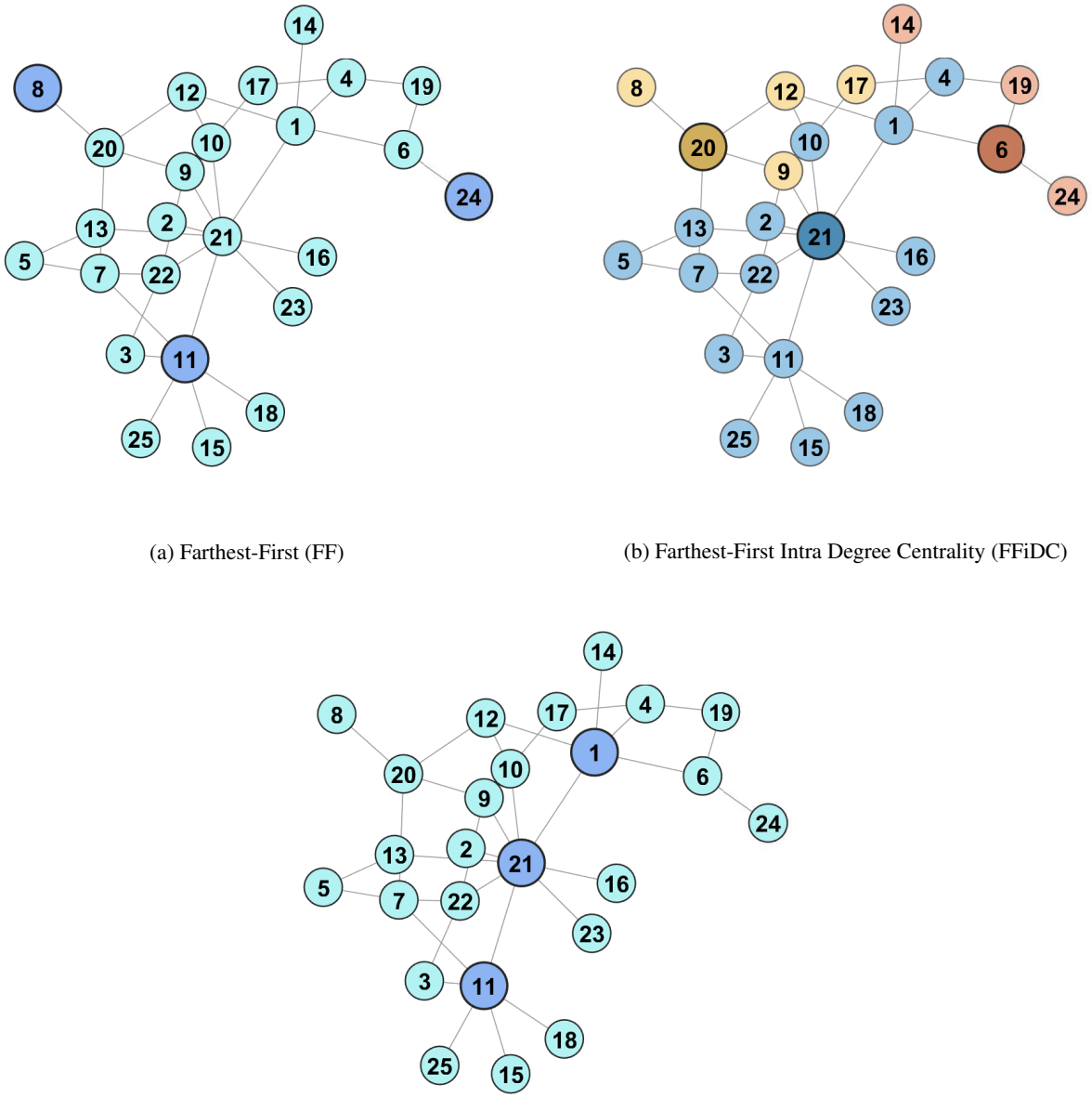
M.R., M.T. and V.S. conceived the study. M.R. and M.T. performed the simulations. M.R., M.T. and V.S. analyzed the results. M.R. and M.T. prepared the figures. M.R., M.T. and V.S. wrote and reviewed the manuscript

Additional information

Funding: No funding was received for this research.

Data availability: The empirical network datasets analyzed in this study are publicly available from the Network Repository. The processed data, simulation results, and code supporting the findings of this study are available from the corresponding author upon reasonable request.

Competing interests: The authors declare no competing interests.



(a) Farthest-First (FF)

(b) Farthest-First Intra Degree Centrality (FFiDC)

(c) Degree Centrality (DC)

Figure 5. Comparison of initial spreader selection strategies in a toy network: (a) FF, (b) FFiDC, and (c) DC. In each case, initial spreaders are highlighted by larger node size and deeper shades. In (b), nodes of the same color belongs to the same partition, and the initial spreader selected corresponds to nodes with the highest intra-degree within the partition.

Supplementary Files

This is a list of supplementary files associated with this preprint. Click to download.

- SupplementaryRTS.pdf